Research Article
https://doi.org/10.1631/jzus.B2400560

A novel drill-milling technology for robot-assisted implant osteotomy preparation: simulation and an *ex vivo* validation study

Chaofan LI[1,2,3], Kangjie CHENG[1,2,3]✉, Chenhao YU[1,2,3], Russell WANG[4], Fudong ZHU[5], Yunfeng LIU[1,2,3]✉

[1]*College of Mechanical Engineering, Zhejiang University of Technology, Hangzhou 310023, China*
[2]*Key Laboratory of Special Purpose Equipment and Advanced Processing Technology, Ministry of Education and Zhejiang Province, Zhejiang University of Technology, Hangzhou 310023, China*
[3]*Collaborative Innovation Center of High-end Laser Manufacturing Equipment (National "2011 Plan"), Zhejiang University of Technology, Hangzhou, 310023, China*
[4]*Department of Comprehensive Care, Case Western Reserve University School of Dental Medicine, Cleveland, OH, 44106-4905, USA*
[5]*Stomatology Hospital, School of Medicine, Zhejiang University, Hangzhou 310006, China*

Abstract: Objective: Excessive frictional heat generated at the drill–bone interface during implant osteotomy can compromise osseointegration and lead to implant failure. This study's objective was to use a helical milling technique for dental implant osteotomy preparation to mitigate thermal damage to the bone. Methods: This study introduces a novel helical milling technique designed to minimize thermal damage to bone during dental implant osteotomy preparations. Finite element simulations were conducted to compare the thermal distribution and cutting stress of a conventional twist drill and the newly designed helical drill. The experimental validation was performed ex vivo on animal bone using a robot-assisted osteotomy system. Results: The finite element simulations revealed that the helical drill produced a maximum cutting stress of 128.9 MPa, higher than the 121 MPa generated by the twist drill, indicating improved cutting efficiency. The ex vivo study demonstrated that the helical milling technique maintained the drilling site temperature below 38.7°C, which was significantly lower than the clinically critical threshold of 47°C and the 61°C recorded with the twist drill. Furthermore, the helical milling process facilitated efficient bone chip removal, reducing thermal buildup. Conclusions: These findings suggest that the helical milling tool and technique optimize robot-assisted osteotomy and effectively mitigate frictional heat generation at the drill–bone interface. This innovation holds promise for enhancing osseointegration success rates in dental implant procedures, offering a clinically viable solution to a long-standing challenge in implantology.

Key words: Drill-milling technology; Robot-assisted drilling; Implant osteotomy preparation; Finite-element analysis; Temperature control

1 Introduction

Oral implantology has been established as a preferred restorative approach for patients with complete and partial edentulism (Buser et al. 2017; Karnik et al. 2024). The initial stage of implant fixture implantation involves proper diagnosis and treatment planning. This is followed by the surgical placement of the implant, involving the creation of an osteotomy site of an appropriate diameter and depth using a serial drilling sequence. This enables an implant fixture to be inserted into the osteotomy site with a desirable insertion torque and primary stability (Yu et al. 2020; Wu et al. 2023). The surgical placement of dental implants using dynamic

✉ Kangjie CHENG, chengkangjie@zjut.edu.cn
Yunfeng LIU, liuyf76@126.com
Chaofan LI, https://orcid.org/0009-0000-7223-4648
Kangjie CHENG, https://orcid.org/0000-0002-2112-0701
Yunfeng LIU, https://orcid.org/0000-0001-8487-0078

Received Nov 5 2024; Revision accepted May 18, 2025;
Crosschecked xxx. xx, 20xx; Published online xxx. xx, 20xx

navigation robots has evolved, and is now more accurate and precise than free-hand implant surgery (Ahmad et al. 2021; Bahrami et al. 2024; X. Sun et al. 2011). The development of automated systems and tools for the robot-assisted surgical insertion of pre-planned implants is complex, sophisticated, and requires further improvement in certain areas.

One of the planned features of future implant robots is the addition of a temperature-cutting force automated system with a haptic feedback function for dental implant drilling preparation. This is critical to the success of dental implant surgery, as elevated temperatures can induce mechanical and thermal damage to the bone (Massoumi et al. 2019). Currently, twist drills are primarily used in clinical practice for osteotomy site preparation. Many factors affect the cutting efficiency of a twist drill; it is commonly cumbersome for removing bone chips from a drilling cavity. The accumulation of bone chips can lead to a significant rise in temperature inside the cavity; if it exceeds 47°C, it may cause thermal necrosis of bone tissue and thus impede osseointegration (Y.-C. Chen et al. 2018). The material and design of a twist drill will further affect the temperature of the surrounding bone tissue during the drilling process (Lee et al. 2018; Lee et al. 2011).

Extensive research has been conducted to address thermal management in bone cavity preparation. Tai et al. (2013) demonstrated that conventional grinding processes generate excessive thermal elevation, with intraosseous temperatures frequently exceeding 100°C in dry cutting conditions. Subsequent innovations have emerged, such as laser-assisted techniques (Shang et al. 2019), although precise energy modulation remains a challenge, potentially inducing osteocyte necrosis. Other recent tool designs show particular promise; for example, Liu et al. (2022) developed a crescent-shaped drill featuring dual cutting edges, which effectively reduced cutting force and improved heat dissipation compared to standard twist drills. Comparative studies by Malvisi et al. (2000) revealed that milling procedures maintain temperatures below 47°C without coolant, outperforming drilling in terms of thermal control, chip removal efficiency, and operational precision. While there are multiple thermal mitigation strategies, this study proposes tool geometry modification combined with advanced thermal monitoring systems as the most viable approach for dental implant cavity preparation. Future work should focus on optimizing cutting tool structure to prevent thermal damage.

Helical milling is a superior method for implant site preparation. The discontinuous contact between the tool and bone, coupled with efficient chip removal, reduces heat generation inside the cavity, thereby minimizing the risk of thermal damage (Barman et al. 2020). The primary advantages of helical milling include significantly reduced cutting forces, smoother cuts due to the gradual engagement of the cutter, improved chip removal, a better surface finish, less tool wear, and the ability to machine a larger range of materials with higher precision. Helical milling technology, widely used in the aerospace field, involves the high-speed rotation of the cutting tool while following a predetermined spiral trajectory, ultimately resulting in the formation of a circular hole larger than the tool's diameter (Dutra Pereira et al. 2017). In orthopedics surgery, bone milling is primarily used to remove abnormal bone tissue or to resect part of the bone material. However, excessive milling forces may lead to fracture and tool breakage during surgery, so it is necessary to model the mechanics of the bone material against milling forces in different directions (Q.-S. Chen et al. 2020). Additionally, milling forces provide valuable intraoperative feedback on bone quality, assisting surgeons in making real-time decisions during the procedure (K. I. Al-Abdullah et al. 2019). Optimizing the milling parameters and controlling the relationship between milling forces and temperature can minimize the damage to bone tissue (Sugita et al. 2009; K. I. A. Al-Abdullah et al. 2018).

Helical milling has the following characteristics: the chips produced are fine and discontinuous; the cutting area is not closed and thus forms a natural chip channel, which can provide improved chip removal and is conducive to the dissipation of heat (H. Wang et al. 2013; Brinksmeier et al. 2011). The processing temperature of helical milling is significantly lower than that of conventional drilling when performing cavity preparation for composite materials (L. Sun et al. 2020). Given the precision and efficiency offered by an implant robotic system, helical milling is considered a viable approach for bone tissue machining.

Due to the complexity of predicting bone tissue temperature during bone tissue milling, more attention has been paid to the study of milling force during milling (Conward & Samuel. 2016; Jiang et al. 2020) However, investigations into strategies for reducing bone tissue temperature by altering the milling technique are limited. In this study, based on the team's previous work (Kan et al. 2022; Cheng et al. 2021), a novel drill-milling tool and a helical cutting process for robot-assisted dental implant site preparation was proposed to mitigate the thermal damage to adjacent bone tissue caused by the use of twist drills. The novel drill-milling tool integrates the helical milling process with a drilling technique, featuring optimized micro-tooth and flute geometry that enhances chip removal efficiency and reduces the cutting temperature. The tool's effectiveness was evaluated with a validation test using ex vivo cavity preparation experiments.

2 Material and methods

2.1 Analysis of heat production in implant site preparing

The heat generated by a chisel edge of a milling cutter during the milling process is similar to that produced by a twist drill cutting. Heat generated by bone milling mainly comes from the friction between fractured bone chips and the cutter surface (G. Chen et al. 2022). If the front face of a cutter is helical, then a contact surface between a chisel edge and bone chips is regarded as a heat source formed along the helical surface by countless line heat sources with different heating intensities. The milling process is depicted in Fig. 1.

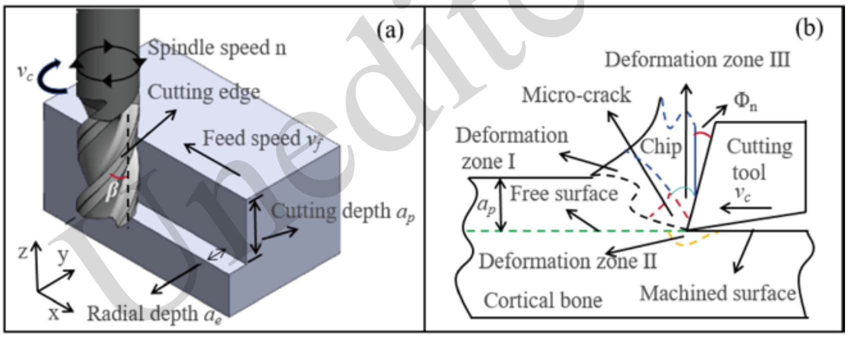

Fig. 1 Milling process. (a) Schematic diagram of the milling operation. (b) Cutting deformation.

The heat generated by the extrusion of side edges with bone chips is Q_{rf}:

$$Q_{rf} = \frac{\tau_s a_p \pi R v_s}{\cos_i \sin \Phi_n \tan_\beta},$$

where β is the helix angle, τ_s is the mandibular shear stress limit value, a_p is the cutting thickness, i is the cutting speed inclination angle, Φ_n is the side edge shear angle, v_s is the shear rate, and R is the cavity radius.

The heat generated by the adhesive friction of the lateral edge with the bone chips is Q_{af}:

$$Q_{af} = \sin \beta_a F_{af} v_c,$$

where β_a is the friction angle, v_c is the cutting speed, and F_{af} is the adhesive friction.

F_{af} is determined by the adhesive friction shear stress τ_n, the axial depth of cut b, and the length of the adhesive contact; assuming that the length of the adhesive contact is l, $F_{af} = \tau_n bl$.

Thus, the heat generated by the adhesive friction of the side blade with the bone chips Q_{af} can be expressed as:

$$Q_{af} = \sin \beta_a \tau_n b l v_c,$$

The relationship between the milling heat of milling cutter formation is:

$$Q = Q_{rf} + Q_{af},$$

In terms of milling heat generation, smaller depths of cut and more uniform cutting force distribution help to reduce heat transfer to the workpiece and the cutting tool. In addition, fractured chips produced by the milling process are discontinuous and discrete. This makes it easier for bone chips to leave the tool, avoiding the phenomenon of bone chip build up. This reduces the friction heat generation between the bone chips and the tool. Therefore, a milling cutter could reduce the temperature rise of bone tissue cutting more than a twist drill.

2.2 Design of drill-milling tool structure

Osteotomy preparation commonly employs conventional twist drills. A twist drill's spiral grooves function to remove bone chips, and the flute width and depth are important elements in facilitating bone chip removal. In the helical milling process, the tool follows a helical path while rotating around its own axis. Low cutting forces, tool wear, and improved borehole quality may be achieved due to its flexible kinematics. Therefore, it is necessary to design a new drill-milling tool for implant osteotomy drilling to provide proper spiral groove and micro-tooth synergistic patterns for effective bone chip removal.

2.2.1 Main structural design

The cutting part of the new drill-milling tool was designed as follows: a 30° bevel angle of the tip, four helical flutes, a 45° helix angle and a 1.5 mm drill diameter. The flute of the drilling and milling tool was designed with a corrugated groove, which could improve reduction of the tool's cutting resistance. The design of the radial angle of the peripheral cutting edge must be considered in terms of cutting sharpness while preventing excessive compressive stress on the bone tissue. The radial front angle of the peripheral cutting edge of the drill-milling tool was -15°, while the radial back angle of the peripheral cutting edge was 15°. The main geometric parameters of the drilling and milling tools are listed in Table 1.

Table 1 Main geometric parameters of the drill-milling tool

Structures	Parameters
Diameter/mm	1.5
Number of teeth	4
Overall length/mm	73.2
Helix angle/°	45
Peripheral rake angle/°	-15
Peripheral Relief Angle/°	15

2.2.2 Micro-tooth structure design

The incorporation of a micro-tooth into the system minimizes bone chip build-up and solves the problem of possible bone chip aggregation at the bend. According to related research (Haddad et al. 2014; Liu et al. 2022), the micro tooth should be 1.778 mm in length, 2.732 mm in width, 1.442 mm of flute width, and with a 45° helix angle. The drill-milling tool is shown in Fig. 2(a). The twist drill used in this experiment is shown in Fig. 2(b). The diameter of the twist drill was 1 mm, the helix angle was 30°, the apex angle was 118°, and the cross-blade angle was 103°.

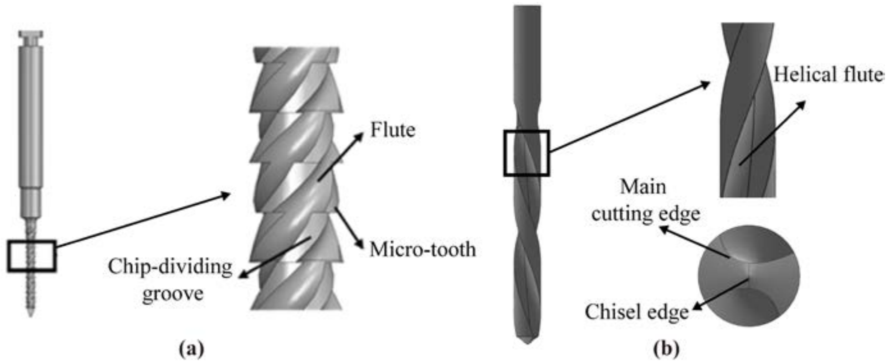

Fig. 2 Geometric structure of cutting tools. (a) Drill-milling tool. (b) Medical twist drill.

2.3 Simulation analysis of bone tissue cutting

2.3.1 Design intent consideration and model preparation

The cavity preparation process for dental implants mainly involves interactions between the tool and the bone. To reduce the calculated time, the model can be simplified without affecting the accuracy of the simulation results. A medical twist drill with a diameter of 3 mm was modelled. The bone model was designed as a cylinder 4.5 mm in diameter and 10 mm in height. Fig. 3 shows two 3D-meshed drill models.

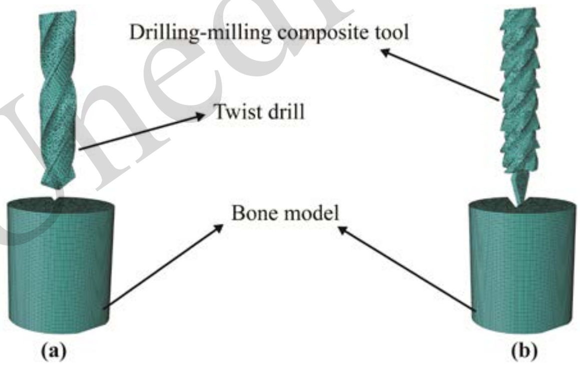

Fig. 3 Tool grid diagram. (a) Twist drill. (b) Drill-milling tool.

2.3.2 Material properties

The material properties of the human jawbone and the drills are listed in Table 2. A simplified Johnson–Cook model (Santiuste et al. 2014; Alam et al. 2009) with material damage criteria was chosen to reflect the material hardening with strain and strain rate during drilling.

Table 2 Material properties of Jawbone and drills.

Material Properties	Jawbone	Twist drill	Drill-milling tool
Density (kg/m^3)	2000	7750	7850
Young's modulus (MPa)	20000	200000	21000
Poisson's ratio	0.36	0.24	0.3
Yield strength（MPa）	56.9	520	585

Johnson–Cook model for flow stresses as follows:

$$\sigma = \left(A + B\varepsilon_1^n\right)\left(1 + C\ln\frac{\varepsilon_2}{\varepsilon_3}\right),$$

where σ is the total flow stress (MPa), A=56.9MPa is the yield stress (MPa), B=101MPa is the work-hardening modulus (MPa), C=0.03 is the strain rate sensitivity coefficient, n =0.08 is the hardening coefficient, ε_1 is the equivalent plastic change, ε_2=0.001s-1 is the plastic strain rate, and ε_3 is the reference plastic strain rate.

2.3.3 Loading and boundary constraints

Face-to-face contact was used in this simulation. The friction coefficient of the penalty function was set to 0.3 in the tangential attribute and hard contact was used in the normal attribute. During the load setting stage, the set kinematic load conditions were applied directly to the reference point. The feed rate of the axial drill loading was 20 mm/min in the negative direction of the Z-axis. The tool drilling speed was 1000 rpm. The lateral cutting load's displacement rate was 40 mm/min in the positive direction of the X-axis, and tool drilling speed was 1000 rpm. Finally, fixed constraints were applied to the six degrees of freedom of the skeleton.

2.4 Bone tissue *in vitro* cavity preparation experiments

2.4.1 Helical milling trajectory planning

Helical milling for implant osteotomy was integrated into a robot-controlled moving arm in a helical trajectory to complete the drilling process. The coordinates of the helical trajectory points were converted to the robot's base coordinate system. The robotic helical milling trajectory motion required the transverse stock removal to be less than a quarter of the tool diameter. Fig. 4 presents a schematic diagram of the spiral trajectory planning.

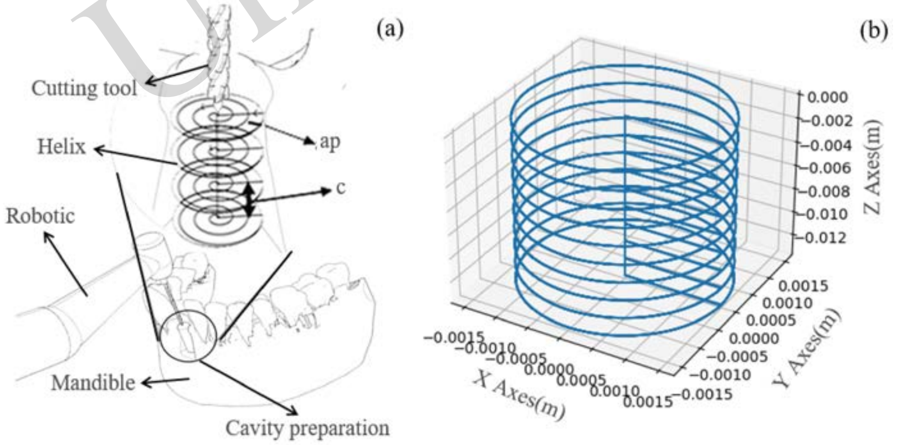

Fig. 4 Schematic diagram of the trajectory planning. (a) Helical milling trajectory. (b) Robotic motion process.

Control of cutting thickness during oral implant osteotomy preparation was achieved using an isometric helix trajectory. Oral implant osteotomy preparation required positioning based on the patient's computed tomography (CT) information. The cavity's center was positioned as the starting point of the isometric helical, then the coordinate system was transformed.

The tool was milled in the plane with the helical trajectory described above and was returned to the starting point of the nest at the end of the movement. Subsequently, the tool moved downwards along the center axis of the cavity. After reaching the target point of the axial feed, the robot repeated the above planar motion.

2.4.2 Experimental material preparation

Fresh beef ribs purchased from the supermarket were cleaned and stored in saline at 4 °C before the experiment. During the experiment, the ribs were cut into small pieces with a diameter of approximately 2.2 cm for clamping with a bench vise on the experimental platform. The cavity preparation experiment is shown in Fig. 5.

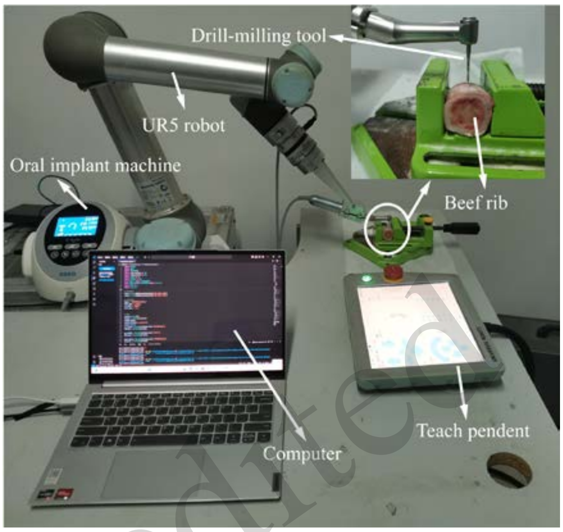

Fig. 5 Cavity preparation experiment.

2.4.3 Cavity preparation experiments *in vitro*

Four thermocouples (K-type, Shanghai Checheng Electromechanical Equipment Co., Ltd, Shanghai, China) were installed around the cavities in a 90° distribution to accurately measure the temperature change of the bone tissue during the milling process as shown in Fig. 6. The robot UR5 prepared four cavities, 0.5 mm in diameter and 2.5 mm in depth, in the rib bone blocks to allow the thermocouple to reside in them for detecting frictional heat during drilling. The distance between the thermocouples and the axial wall of a final prepared drilling site was 0.5 mm. The cavities, where the thermocouples were pre-buried, were filled with thermally conductive silicone grease to reduce the effect of heat transfer with the surrounding air and other media. The thermocouple wires were inserted into the cavity at the same depth and fixed to ensure the stability of temperature measurement during cavity preparation.

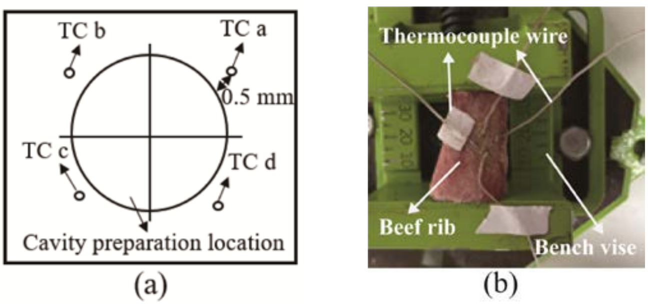

Fig. 6 Thermocouple position. (a) Schematic drawing of thermocouple distribution. (b) Bone sample with fixed thermocouple wires.

Two groups were created: a control group, for which conventional twist drilling was employed, and an experimental group, for which a helical milling technique was applied using a drill-milling tool. For both groups, the drills' rotation speed was set to 1000 rpm, the diameter and depth of the prepared cavities were 3 mm and 10 mm, respectively, the helical milling's rotational velocity of was 1 rpm, and the feed rate of the twist drill in the control group was 20 mm/min.

3 Results

3.1 Simulation of bone tissue cutting

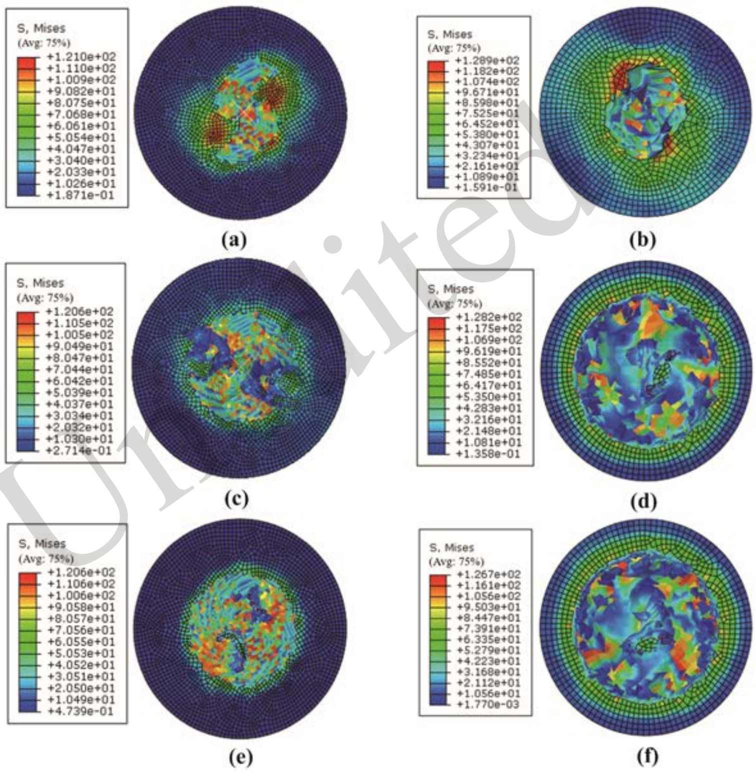

Fig. 7 Equivalent stress diagram of bone tissue. 0.25 s (a,b), 2.5 s (c,d), 5 s (e,f). The left column represents the medical twisted drill. The right column represents the drill-milling tool.

Three time points-0.25 s, 2.5 s, and 5 s-were selected to analyze the cutting effect. Fig. 7 illustrates that the stress generated by the drill-milling tool consistently exceeded that of the twist drill at all observed moments. At 5 s, the maximum stress generated by the drill-milling tool and the twist drill was 128.9 MPa and 121 MPa, respectively.

Fig. 8 shows the variation in axial force during the cutting process of the extracted bone tissue at different moments. The axial force increased continuously in the initial seconds and then exhibited a periodic change. The twist drill consistently produced higher axial forces than the drill-milling tool, with a peak axial force of 22 N occurring within the first 0.5 s. In contrast, the drill-milling tool demonstrated a more gradual increase in axial force, reaching a maximum value of 10.5 N within 3 s.

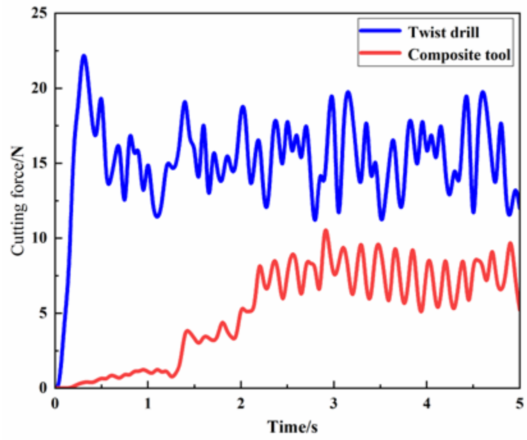

Fig. 8 Axial force variation during drilling process by twist drill and composite tool.

3.2 *Ex vivo* cavity preparation study

Real time temperature data were collected by the thermocouples during the cutting process with the drill-milling tool. The temperature data measured by thermocouples at different positions vary over time, as shown in Figs. 9(a)-(b). It can be observed that the temperature around the cavity exhibited an increasing then decreasing trend. The average temperatures measured by the thermocouples were compared with those recorded during twist drill cutting as shown in Fig. 9(d). The maximum temperature reached during helical milling was 38.7°C, significantly lower than the 61°C observed during twist drilling. Additionally, the bone chips were successfully evacuated around the cavity when cutting with the drill-milling tool, as shown in Fig. 10.

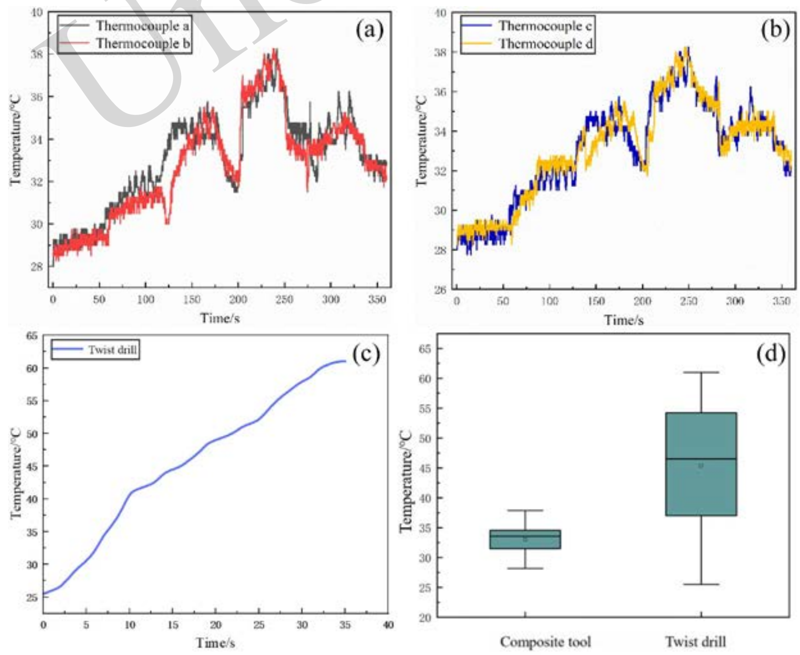

Fig. 9 Temperature change. Thermocouple temperature recorded by drill-milling tool (a,b). (c) Temperature change by twist drill. (d) Temperature comparison from cavity preparations with different tools.

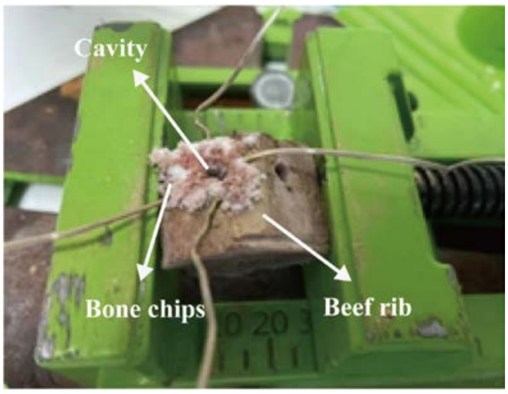

Fig. 10 Bone chips discharged from the cavity.

4 Discussion

Versatile cutting tools are available in multiple point angles and are perfect for drilling, grooving, milling, spotting, and chamfering (Park et al. 2010). While milling employs sideways motions to cut the material, drilling uses up-and-down actions. During dental implant site preparation, the heat generated by cutting is transferred to the bone, resulting in rising bone temperature (Karmani. 2006). The elevated temperatures compromise the osseointegration process, potentially leading to implant failure. In this study, a drill-milling tool was developed for implant robots to address thermal damage. Cavity preparation experiments conducted on beef ribs demonstrated that this tool effectively reduced the temperature around the cavity.

4.1 Simulation of bone tissue cutting

From the stress distribution at the moment t=0.25 s, it could be observed that the maximum stress was generated at the tip of the drill at the time when the chisel edge of the main cutting part of the drill-milling tool contacted the cortical bone. With the continuous movement of the drill-milling tool, the stress field was further extended, while the maximum stress gradually appeared around the drilled cavity. When the stress–strain reached a critical point, the bone started to deform plastically. Fractured chips were formed when the limit value of the bone tissue was reached. Research has demonstrated that contact between the drill bit and the bone surface induces stress, leading to initial linear elastic deformation (Isbilir & Ghassemieh. 2012).

Cutting force is an important index for evaluating machining performance, as its fluctuations affect cutting quality (T. Chen et al. 2023). Drill-milling tool cutting will produce a large equivalent force. Increasing cutting stress to a certain extent was beneficial for improving the efficiency of cavity preparation and reducing bone tissue damage (Su, Hu, et al. 2020; Su, Li, et al. 2020). The overall drilling process showed that the equivalent stress values in the bone region of the drill-milling tool were similar to those of the twist drill, which were less than the limiting stress value of 150 MPa in human bone (Huang et al. 2019). Therefore, the milling of bone tissue using drill-milling tools did not rupture the surrounding bone wall.

An axial force was generated upon contact between the rotating tool and the bone tissue, which progressively increased as the axial cutting process advanced. The increase in axial force was slower in drill-milling tools due to their micro-tooth structure. The trajectory of the tool was helical throughout the process. The increase in cutting depth caused by the tool was subjected to the same axial force; therefore, the axial force varied at different time intervals. For the drill-milling tool, the lower axial force during drilling could improve drilling defects (Turki et al. 2014; Su et al. 2021). In the present study's experiments, the average value of the axial force generated by the drill-milling tool during cutting was 8.1 N, which was less than the average value of the axial force of the twist drill (14.7 N). This demonstrated that the drill-milling tool cutting could form a better-quality prepared cavity.

4.2 *Ex vivo* cavity preparation study

The temperature tended to increase linearly when the tool rotated near the thermocouple temperature measurement point as shown in Fig. 9(a) and (b). As the tool moved away from the thermocouple point with the helical milling motion, the temperature decreased further, exhibiting good heat dissipation characteristics. Comparing the temperature variations of the four thermocouples revealed clear periodic variations in the temperature rise. The regular discontinuous variation of chips during milling also caused the cutting force and cutting temperature to vary at different time intervals rather than remaining in a steady state (Chang. 2007).

Since the milling motion took 60 s for one round, compared to the temperature trend in thermocouple a, the second temperature rise in thermocouple b showed a delay of about 15 s. Similar situations occurred in thermocouples c and d. There might be some sudden temperature increases or decreases across the temperature variations depicted in Fig. 9(a) and (b), due to the influence of environmental factors. Overall, the trend of the temperature profile was approximately the same, which aligned with the expected cyclic change pattern.

Throughout the cutting process, the maximum temperature of the helical milled cavity preparation was much lower than that of the twist drill drilling. This was because the bone chips did not build up during helical milling cavity preparation as they did with twist drilling, as shown in Fig. 10. Bone chip evacuation helped the tool to dissipate heat during idle travel (Y. Wang et al. 2022; Barry & Byrne. 2002)

The drill-milling tool reduced the friction heat between the bone chips and the tool by reducing the accumulation of bone chips in the cavity, resulting in the discharge of bone chips, transferring some of the heat out of the cavity.

The results demonstrated that the drill-milling tool significantly reduced bone tissue temperature during cavity preparation, confirming both the feasibility and effectiveness of helical milling for dental implant site preparation. Additionally, this technique demonstrated obvious advantages in mitigating thermal damage to bone tissue. However, the temperature data in this study did not take into account the thermal diffusion in the surrounding bone tissue, introducing slight errors. Future work will involve developing a heat diffusion model to correct the measured temperature data for improved prediction of heat transfer during cavity preparation. In addition, future research and parameter optimization can be conducted on the milling cavity preparation process on the basis of the robot cavity preparation milling process proposed in this article.

5 Conclusions

In this research, a novel drill-milling technology was developed for robot-assisted helical milling to mitigate thermal damage to bone tissue during implant site drilling by dental implant robots. The main conclusions were as follows:

(1) The principle of cutting heat generation in the process of cavity preparation for planting was analyzed, and a composite drilling-milling tool was prepared by combining the advantages of robot and helical milling. Due to the micro-tooth structure, the drill-milling technology demonstrated effective bone chip evacuation during the machining process, creating a good heat dissipation environment. The maximum temperature of the cavity preparation control was 38.7°C, and the issue of increasing temperature was effectively controlled.

(2) Compared to twist drills, the higher cutting stress of the milling-drilling tool helped to increase the efficiency of cavity preparation and thus reduced the risk of bone tissue damage.

(3) The maximum temperature during helical milling remained well within the safe range for bone cell survival. The experimental results confirm the practical viability of the helical milling technique for implant osteotomy preparations and offer valuable technical insights for future optimization of robotic-assisted oral implant surgery.

Data availability statement

The dataset used or analyzed during the current study is available from the corresponding author on reasonable request.

Acknowledgments

This work was financially supported by the National Natural Science Foundation of China (Grant No: 52175280, 52305326), the Zhejiang Provincial Natural Science Foundation of China (Grant No: LQ23E050016) and the 111 Project (No. D16004)

Author contributions

Conceptualization and writing–original draft preparation were performed by Chaofan LI; Writing–review and editing and investigation were performed by Kangjie CHENG, Russell WANG and Fudong ZHU; Chenhao YU interpreted data; Methodology and funding acquisition were performed by Yunfeng LIU. All authors read and approved the final manuscript and, therefore, had full access to all the data in the study and take responsibility for the integrity and security of the data.

Compliance with ethics guidelines

Chaofan LI, Kangjie CHENG, Russell WANG, Fudong ZHU, Chenhao YU and Yunfeng LIU declare that they have no conflicts of interest.

This review does not contain any studies with human or animal subjects performed by any of the authors.

All authors agree to publish in the Journal of Zhejiang University-SCIENCE B (Biomedicine & Biotechnology).

References

Ahmad P., Alam MK., Aldajani A., et al., 2021. Dental Robotics: A Disruptive Technology. Sensors, 21(10), 3308. https://doi.org/10.3390/s21103308.

Al-Abdullah K IA, Abdi H, Lim CP, et al., 2018. Force and temperature modelling of bone milling using artificial neural networks. Measurement, 116, 25–37. https://doi.org/10.1016/j.measurement.2017.10.051.

Al-Abdullah KI, Lim CP, Najdovski Z, et al., 2019. A model-based bone milling state identification method via force sensing for a robotic surgical system. Int J Med Robot Comp, 15(3). https://doi.org/10.1002/rcs.1989.

Alam K, Mitrofanov AV, Silberschmidt VV, 2009. Finite element analysis of forces of plane cutting of cortical bone. Comput. Mater. Sci, 46(3), 738–743. https://doi.org/10.1016/j.commatsci.2009.04.035.

Bahrami R, Pourhajibagher M, Nikparto N, et al, 2024. Robot-assisted dental implant surgery procedure: A literature review. J Dent Sci, 19(3), 1359–1368. https://doi.org/10.1016/j.jds.2024.03.011.

Barman A., Adhikari R., Bolar G, 2020. Evaluation of conventional drilling and helical milling for processing of holes in titanium alloy Ti6Al4V. MTProceedings, 28, 2295–2300. https://doi.org/10.1016/j.matpr.2020.04.573.

Barry J, Byrne G, 2002, The mechanisms of chip formation in machining hardened steels. J. Manuf. Sci. Eng, 124(3), 528–535. https://doi.org/10.1115/1.1455643.

Brinksmeier E., Fangmann S., Rentsch R, 2011. Drilling of composites and resulting surface integrity. CIRP Ann-Manuf Techn, 60(1), 57–60. https://doi.org/10.1016/j.cirp.2011.03.077.

Buser D., Sennerby L, De Bruyn H, 2017. Modern implant dentistry based on osseointegration: 50 years of progress, current trends and open questions. Periodontol. 2000, 73(1), 7–21. https://doi.org/10.1111/prd.12185.

Chang, CS, 2007. Prediction of the cutting temperatures of stainless steel with chamfered main cutting edge tools. J. Mater. Process. Technol, 190(1–3), 332–341. https://doi.org/10.1016/j.jmatprotec.2007.02.020.

Chen G, Gao Q, Yang X, et al, 2022. Investigation of heat partition and instantaneous temperature in milling of Ti-6Al-4V alloy. J. Manuf. Process, 80, 302–319. https://doi.org/10.1016/j.jmapro.2022.05.051.

Chen QS, Dai L, Liu Y, et al, 2020. A cortical bone milling force model based on orthogonal cutting distribution method. Adv. Manuf, 8(2), 204–215. https://doi.org/10.1007/s40436-020-00300-7.

Chen T, Liu J, Liu G, et al, 2023. Experimental Study on Titanium Alloy Cutting Property and Wear Mechanism with Circular-arc Milling Cutters. Chin. J. Mech. Eng, 36(1), 57. https://doi.org/10.1186/s10033-023-00887-5.

Chen YC, Tu YK, Tsai YJ, et al, 2018. Assessment of thermal necrosis risk regions for different bone qualities as a function of

drilling parameters. Comput. Meth. Programs Biomed, 162, 253–261.
https://doi.org/10.1016/j.cmpb.2018.05.018.

Cheng KJ, Kan TS, Liu YF, et al., 2021. Accuracy of dental implant surgery with robotic position feedback and registration algorithm: An in-vitro study. Comput. Biol. Med, 129, 104153.
https://doi.org/10.1016/j.compbiomed.2020.104153.

Conward M, Samuel J, 2016. Machining characteristics of the haversian and plexiform components of bovine cortical bone. J. Mech. Behav. Biomed. Mater, 60, 525–534.
https://doi.org/10.1016/j.jmbbm.2016.03.017.

Haddad M, Zitoune R, Eyma F, et al., 2014. Study of the surface defects and dust generated during trimming of CFRP: Influence of tool geometry, machining parameters and cutting speed range. Compos Part A-Appl S, 66, 142–154.
https://doi.org/10.1016/j.compositesa.2014.07.005.

Haiyan W, Xuda Q, Hao L, et al., 2013. Analysis of cutting forces in helical milling of carbon fiber-reinforced plastics. P I MECH ENG B-J ENG, 227(B1), 62–74.
https://doi.org/10.1177/0954405412464328.

Huang SN, Shie MY, Shen YW, et al., 2019. Biomechanical Assessment of Design Parameters on a Self-Developed 3D-Printed Titanium-Alloy Reconstruction/Prosthetic Implant for Mandibular Segmental Osteotomy Defect. Metals, 9(5), 597.
https://doi.org/10.3390/met9050597.

Isbilir O, Ghassemieh E, 2012. Finite Element Analysis of Drilling of Carbon Fibre Reinforced Composites. Appl Compos Mater, 19(3–4), 637–656.
https://doi.org/10.1007/s10443-011-9224-9.

Jiang Z, Qi X, Sun Y, et al., 2020. Cutting Depth Monitoring Based on Milling Force for Robot-Assisted Laminectomy. IEEE Trans. Autom. Sci. Eng, 17(1), 2–14.
https://doi.org/10.1109/TASE.2019.2920133.

Kan TS, Cheng KJ, Liu YF, et al., 2022. Evaluation of a custom-designed human-robot collaboration control system for dental implant robot. Int J Med Robot Comp, 18(1), e2346.
https://doi.org/10.1002/rcs.2346.

Karmani, S, 2006. The thermal properties of bone and the effects of surgical intervention. Curr. Orthop 20(1), 52–58.
https://doi.org/10.1016/j.cuor.2005.09.011.

Karnik AP., Chhajer H., Venkatesh, SB, 2024. Transforming Prosthodontics and oral implantology using robotics and artificial intelligence. Frontiers Oral Health, 5, 1442100.
https://doi.org/10.3389/froh.2024.1442100.

Lee J, Chavez, C. L, Park J, 2018. Parameters affecting mechanical and thermal responses in bone drilling: A review. J. Biomech, 71, 4–21.
https://doi.org/10.1016/j.jbiomech.2018.02.025.

Lee J, Rabin Y, Ozdoganlar OB, 2011. A new thermal model for bone drilling with applications to orthopaedic surgery. Med. Eng. Phys, 33(10), 1234–1244.
https://doi.org/10.1016/j.medengphy.2011.05.014.

Liu J, Tang X, Li S, et al., 2022. Optimization of multi-tooth milling tool for interlaminar damage suppression in the milling of carbon fiber-reinforced polymers. Int J Adv Manuf Technol, 121(1–2), 1235–1251.
https://doi.org/10.1007/s00170-022-09369-9.

Liu S, Wu D, Zhao J, et al.,2022. Novel crescent drill design and mechanistic force modeling for thrust force reduction in bone drilling. Med Eng Phys,103, 103795.
https://doi.org/10.1016/j.medengphy.2022.103795.

Malvisi A., Vendruscolo P., Morici F.,et al., 2000. Milling versus sawing: comparison of temperature elevation and clinical performance during bone cutting. In International conference on medical image computing and computer-assisted intervention, p.1238-1244.
https://doi.org/10.1007/978-3-540-40899-4_133.

Massoumi F, Tafti AA, Mirdehghan SM, 2019. Heat Caused by Dental Implant Fixture Seating: Temperature In Vitro and Software Simulation. J. Long-Term Eff. Med. Implants, 29(4), 303–310.
https://doi.org/10.1615/JLongTermEffMedImplants.2020033868.

Park SY, Shin SY, Yang SM, et al., 2010. Effect of implant drill design on the particle size of the bone collected during osteotomy. Int. J. Oral Maxillofac. Surg., 39(10), 1007–1011.
https://doi.org/10.1016/j.ijom.2010.05.009.

Pereira R BD, Brandão LC, de Paiva AP, et al., 2017. A review of helical milling process. Int. J. Mach. Tools Manuf, 120, 27–48.
https://doi.org/10.1016/j.ijmachtools.2017.05.002.

Santiuste C, Rodríguez-Millán M, Giner E, et al., 2014. The influence of anisotropy in numerical modeling of orthogonal cutting

of cortical bone. Compos. Struct, 116(9), 423–431. https://doi.org/10.1016/j.compstruct.2014.05.031.
Shang Z., Liao Z., Sarasua J. A, et al., 2019. On modelling of laser assisted machining: Forward and inverse problems for heat placement control. Int J Mach Tool Manu,138, 36-50. https://doi.org/10.1016/j.ijmachtools.2018.12.001.
Su F, Hu Z, Rong Z, et al., 2020. New drill-milling tools for novel drill-milling process of carbon fiber-reinforced plastics. Int J Adv Manuf Technol., 107(1–2), 217–228. https://doi.org/10.1007/s00170-020-05092-5.
Su F, Li C, Li W, et al., 2020. Cutting forces and correlation with the damages during CFRP drill-milling by using novel drill-milling tool. Int J Adv Manuf Technol, 108(7–8), 2661–2674. https://doi.org/10.1007/s00170-020-05580-8.
Su F, Li W, Juan C, et al., 2021. Drill-milling process and novel drill-milling tool for making a hole on carbon fiber-reinforced plastics. Int J Adv Manuf Technol, 115(7–8), 2125–2143. https://doi.org/10.1007/s00170-021-07110-6.
Sugita N, Osa, T, Mitsuishi M, 2009. Analysis and estimation of cutting-temperature distribution during end milling in relation to orthopedic surgery. Med. Eng. Phys, 31(1), 101–107. https://doi.org/10.1016/j.medengphy.2008.05.001.
Sun L, Gao H, Wang B, et al., 2020. Mechanism of reduction of damage during helical milling of titanium/CFRP/aluminium stacks. Int J Adv Manuf Technol, 107(11–12), 4741–4753. https://doi.org/10.1007/s00170-020-05177-1.
Sun X, McKenzie FD, Bawab S, et al., 2011. Automated dental implantation using image-guided robotics: Registration results. Int. J. Comput. Assist. Radiol. Surg, 6(5), 627–634. https://doi.org/10.1007/s11548-010-0543-3.
Tai BL, Zhang L, Wang A, et al., 2013. Neurosurgical bone grinding temperature monitoring.Procedia Cirp,5, 226-230. https://doi.org/10.1016/j.procir.2013.01.045.
Turki Y, Habak M, Velasco R, et al., 2014. Experimental investigation of drilling damage and stitching effects on the mechanical behavior of carbon/epoxy composites. Int. J. Mach. Tools Manuf, 87, 61–72. https://doi.org/10.1016/j.ijmachtools.2014.06.004.
Wang Y, Li J, Liu K, et al., 2022. Experiment and numerical study of chip formation mechanism during cryogenic machining of Ti-6Al-4V alloy. J. Manuf. Process, 84, 1246–1257. https://doi.org/10.1016/j.jmapro.2022.10.020.
Wu H, Chen X, Kong L, et al., 2023. Mechanical and Biological Properties of Titanium and Its Alloys for Oral Implant with Preparation Techniques: A Review. Materlals, 16(21), 6860. https://doi.org/10.3390/ma16216860.
Yu D, Liu C, Wu Y, et al., 2020. Measurement and prediction of drilling force in fresh human cadaver mandibles: A pilot study. Clin. Implant Dent. Relat. Res, 22(1), 4–12. https://doi.org/10.1111/cid.12841